Multi-carrier 1.44-Tb/s Silicon Photonic Coherent Receiver using IQ Imbalance Compensation

Zhen Wang
State Key Lab of Advanced Optical Communication Systems and Networks
Department of Electronic Engineering, Shanghai Jiao Tong University
Shanghai, China
njwz526@sjtu.edu.cn

Xingfeng Li
State Key Lab of Advanced Optical Communication Systems and Networks
Department of Electronic Engineering, Shanghai Jiao Tong University
Shanghai, China
xingfengli@sjtu.edu.cn

Shuo Wang
State Key Lab of Advanced Optical Communication Systems and Networks
Department of Electronic Engineering, Shanghai Jiao Tong University
Shanghai, China
shuo.wang@sjtu.edu.cn

Jian Shen
State Key Lab of Advanced Optical Communication Systems and Networks
Department of Electronic Engineering, Shanghai Jiao Tong University
Shanghai, China
jian_shen@sjtu.edu.cn

Yong Zhang
State Key Lab of Advanced Optical Communication Systems and Networks
Department of Electronic Engineering, Shanghai Jiao Tong University
Shanghai, China
yongzhang@sjtu.edu.cn

Yikai SU
State Key Lab of Advanced Optical Communication Systems and Networks
Department of Electronic Engineering, Shanghai Jiao Tong University
Shanghai, China
yikaisu@sjtu.edu.cn

2023 Opto-Electronics and Communications Conference (OECC) | 978-1-6654-6213-6/23/$31.00 ©2023 IEEE | DOI: 10.1109/OECC56963.2023.10209574

***Abstract*—We present a polarization-diversity coherent receiver that enables wavelength-multiplexed reception without arrayed waveguide gratings. We compensate in-phase and quadrature imbalance using a MIMO equalizer, enabling a 1.44-Tb/s capacity of wavelength-division-multiplexed and polarization-division-multiplexed 16-ary quadrature-amplitude-modulation signals.**

Keywords—silicon photonics, optical receivers, coherent communication, WDM, PDM

I. Introduction

Optical transmission systems have made remarkable progress in recent years, achieving higher spectral efficiencies and data rates, and lower costs [1]-[12]. These advancements have been achieved by employing wavelength-division multiplexing (WDM) and polarization-division multiplexing (PDM) techniques, along with the adoption of advanced optical modulation formats. In particular, coherent optical transmission has become a critical technology for high-capacity and long-haul communications, enabling channel data rates exceeding 100 Gb/s [3],[13]-[20]. The latest 200/400-Gb/s networks have successfully employed polarization-division-multiplexed 16-quadrature amplitude modulation (16-QAM) [19], [21]-[22].

Silicon-on-insulator platform is a promising option for compact and cost-effective integrated coherent transceivers, owing to the high refractive index contrast of the materials [23]. A typical method for detecting WDM-PDM signals is to use an arrayed waveguide grating (AWG) to separate the WDM signals in the frequency domain, and a polarization splitter and rotator (PSR) to separate the PDM signals based on polarization. Then, the de-multiplexed signals are input to 90° hybrids with the local oscillator (LO) [24], [25]. Due to the beating effect in the photodiode (PD), the signal in the frequency domain would be shifted based on the frequency of the LO, which allows for coherent detection of WDM signals without the need for WDM de-multiplexing. Therefore, considerable space required for AWG can be saved. Nevertheless, due to the imperfection of the transmitter (Tx), the IQ imbalance cannot be entirely eliminated and the resulting crosstalk and signal-signal beat interference (SSBI) are added to the photocurrents. To address this issue, a real-value 2×2 multiple-input and multiple-output (MIMO) equalizer was proposed to compensate for IQ imbalance [26]. In WDM coherent detection without an AWG, this technique can effectively eliminate the crosstalk and SSBIs caused by the beating effect between different wavelength signals.

Recently, we proposed and demonstrated an AWG-free coherent receiver to detect 1.12Tb/s DWDM-PDM-16QAM signals [27]. Low-pass filters are used to filter out the high-frequency noise generated by mixing the LO with signals at other wavelengths resulting from the absence of AWG. However, the baud rate was limited to 28-GBaud, which may not satisfy the high-capacity demand. In this paper, we increase the baud rate to 36-GBaud while compensating for the IQ imbalance caused by the imperfect of Tx and the unequal responsivities of the on-chip PD using a 2×2 MIMO-FFE. We experimentally demonstrate coherent detection of 1.44-Tb/s dense wavelength-division multiplexed (DWDM) and PDM signals using an integrated silicon coherent receiver without an AWG.

II. Principle

To address the issue of large footprint of AWGs in WDM coherent receivers[28], we presented an AWG-free coherent receiver based on the SOI platform [27]. As illustrated in Fig. 1(a), the LO light (C, take λ_1 as the channel-under-test (CUT)) and signals on five wavelengths (S_n, $\lambda_1 \sim \lambda_5$) are hybridized in a 90° hybrid based on the 4×4 multi-mode interferometer (MMI) without the presence of an AWG for wavelength demultiplexing. The lights are received and mixed in the GePDs, followed by low-pass filtering to remove high-frequency noise [27]. However, due to the imperfection of the transmitter and the unequal responsivities of the GePDs, the photocurrents received by GePDs are:

$$S_n = I_n + j\alpha_n Q_n\left(t-\Delta t_n\right)e^{j\theta_n}, \tag{1}$$

National Natural Science Foundation of China (Grant Nos. 61835008, 61860206001, and 61975115).

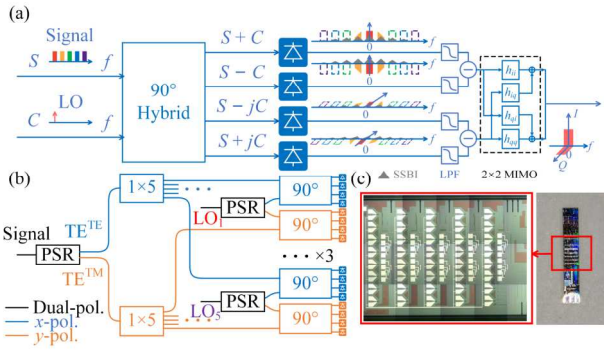

Fig. 1 (a) The hybrid and detection of DWDM signals in our proposed coherent receiver (take λ_1 as the CUT). Due to the bandwidth limitations of germanium PDs (GePDs), probes, and cables, only signals with frequencies below 50-GHz can be detected, (b) the block diagram. (c) microscope photographs.

where S is the signal while I and Q are the in-phase and quadrature components (normalized to I). n represents different wavelengths. α, Δt, and θ denote amplitude mismatch, time delay, and phase mismatch, respectively. Thus, the resulting photocurrents of the base-band signals are interfered with the crosstalk scaled by $\alpha\sin(\theta_n)$ to the Q component as the last term in the right side of Eq. (2):

$$\begin{aligned} I_1 &= \frac{1}{2}\left|C+\sum_{n=1}^{5}\left(I_n + j\alpha_n Q_n\left(t-\Delta t_n\right)e^{j\theta_n}\right)\right|^2 \\ &= \frac{1}{2}\left|C+\sum_{n=1}^{5}\left(I_n + j\alpha_n Q_n\left(t-\Delta t_n\right)\cos\left(\theta_n\right)\right.\right. \\ &\quad \left.\left. -\alpha_n Q_n\left(t-\Delta t_n\right)\sin\left(\theta_n\right)\right)\right|^2, \end{aligned} \tag{2}$$

As for the imaginary part of the signal, it is impaired in amplitude ($\alpha\cos(\theta_n)$) and has a time delay of Δt. Similarly, the crosstalk in Q component is introduced by the I component of the signal. To eliminate the crosstalk introduced by IQ imbalance, we use a butterfly-structured 2×2 MIMO equalizer as follows [26]:

$$\begin{aligned} y_i(n) &= \sum_{k=0}^{N-1} h_{ii}(n)\,x_i(n-k) + \sum_{k=0}^{N-1} h_{iq}(n)\,x_q(n-k), \\ y_q(n) &= \sum_{k=0}^{N-1} h_{qi}(n)\,x_i(n-k) + \sum_{k=0}^{N-1} h_{qq}(n)\,x_q(n-k), \end{aligned} \tag{3}$$

where h_{ii}, h_{iq}, h_{qi} and h_{qq} are four finite impulse response filters, and N is the tap length.

III. Structural Design and Fabrication

The proposed silicon coherent receiver integrates all the necessary components for interconnecting photonics elements, such as GePDs, edge couplers (ECs), and PSRs. Fig. 1(b) and (c) provide a block diagram and microscope photographs of the fabricated receiver, respectively. This receiver comprises six edge couplers, six PSRs, ten 4×4 MMIs, and forty GePDs, with an overall footprint of 3.87 mm × 2.8 mm. The chip was fabricated on an SOI wafer with a 220-nm top silicon layer at the Advanced Micro Foundry (AMF, Singapore).

The optical signal, consisting of five wavelengths ($\lambda_1 \sim \lambda_5$) with two polarizations, is fed into the signal port on one side of the chip, while five LO lights are coupled into the silicon chip through the LO ports on the other side of the chip. The wavelengths of five input LOs can be out of order since the wavelengths of signal demodulated in each 90° hybrid are selected by the wavelengths of the input LOs. The polarization multiplexed signal and 45°-polarized LO lights (which can be decomposed into x- and y-polarizations) are divided and converted into TE polarizations through six PSRs (one for signal, five for LO). Two TE-polarized signal lights converted from different polarizations are respectively split into five beams by two three-stage 1×2 coupler arrays and then input to ten 4×4 MMIs, whose four output lights are absorbed by four GePDs. The balanced detection and the IQ imbalance compensation are performed in digital signal processing (DSP).

IV. Experimental Setup and Results

Fig. 2(a) depicts a back-to-back experimental setup for testing the proposed coherent receiver. At the transmitter side, a continuous-wave (CW) light from a tunable laser source (TLS) (SOUTHERN PHOTONICS TLS150) was amplified to 18 dBm using an erbium-doped fiber amplifier (EDFA) and launched to a commercial in-phase and quadrature modulator (IQM) [6]. The IQM was driven by a 36-GBaud Nyquist 16-QAM signal from a 100 GSa/s digital-to-analog converter (MICRAM DAC 10002). Due to the limited number of CW lasers available, we used a wave shaper on another branch to spectrally shape an ASE source [29], [30]. A 2×2 polarization-maintaining coupler combined the spectrally shaped signal with the modulated signal to emulate the 5 DWDM channels with 50-GHz spacing. Then, the DWDM signals were divided into two copies, and a fiber delay line was utilized to decorrelate the two copies. After that, a polarization beam combiner (PBC) combined two decorrelated copies to generate a PDM signal. Figs. 2(b~f) present the optical spectrum after DWDM and PDM. Thus, five 288-Gb/s PDM 16-ary quadrature amplitude modulation (16-QAM) signals at five wavelengths were generated and sent into the proposed coherent receiver.

At the receiver side, the generated DWDM-PDM signal was amplified by the $EDFA_3$ before being launched into the coherent receiver. Since we only have one four-channel digital storage oscilloscope (DSO) (LeCroy 36Zi-A), we can only

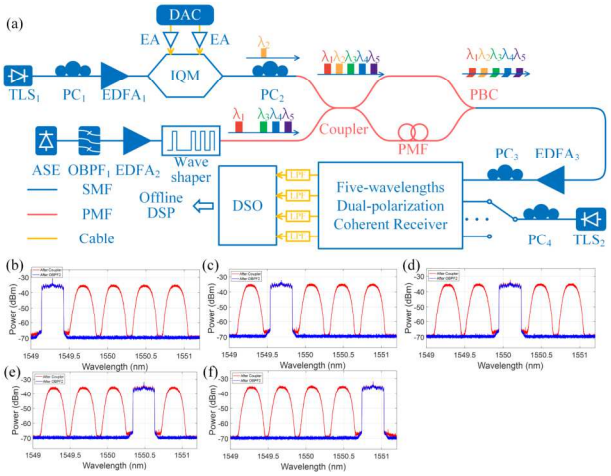

Fig. 2 (a) Schematic of the experimental setup for generation and detection of the coherent communication system performance. (b~f) The optical spectra of the generated signals of different CUT, the lights on other wavelengths are ASE noise. The spectra of the two polarizations are identical.

receive a single-polarization signal at a time. We used two polarization controllers (PC_3 and PC_4) to align the polarization states between the signal and the LO. Due to the presence of the PSR, this method is equivalent to inputting 45°-polarized light with twice the intensity. The wavelength of the LO is coarsely aligned with that of the CUT. To achieve larger output powers from the 90° hybrids, the optical power of the LO is set to 10 dBm. Four Bias-Tees supply the −2-V bias voltages for the four on-chip GePDs. The received optical signals are converted to electrical signals and filtered to eliminate the high-frequency components to forestall spectral aliasing. Finally, the obtained electrical is recorded by an 80-GSa/s DSO and processed offline using DSP.

Fig. 3 outlines the flow chart of the DSP algorithms utilized at both the transmitter and receiver. At the transmitter, binary data is mapped to 16-QAM symbols, the synchronization and training sequences are added at the head of the payload, and the signal pulse is shaped by a root-raised cosine (RRC) filter with a roll-off factor of 0.01. Pre-emphasis is implemented to compensate for the imperfect frequency response of the transmitter-side components. After being resampled to 100 GSa/s, the signals are clipped to suppress the peak-to-power ratio for fully utilizing the dynamic range of the DAC. On the receiver side, the function of balanced detection is achieved in DSP. After frequency offset compensation (FOC) and synchronization, a 2×2 MIMO-FFE is utilized to compensate IQ imbalance and mitigate inter-symbol interference (ISI) since the responsivities of the GePDs are not identical. The carrier phase recovery is realized using a blind phase search (BPS) algorithm. Then, we use a post filter to minimize the influence of the noise enhancement effect of the FFE, and the maximum likelihood sequence detection (MLSD) is employed for symbol recovery. After de-mapping, the bit error ratio (BER) is calculated.

After obtaining the x-polarization signal at wavelength λ_1, we moved the radio frequency probe array to the pads associated with the y-polarization, adjusted the PC_4 to the opposite polarization, and changed the output wavelengths of both TLSs to λ_2. We then adjusted the wave shaper setting to suppress the light at λ_2 and proceeded with the dual polarization data sampling process. We repeated this process ten times to acquire data for all ten channels of the DWDM-PDM 16-QAM optical communication system.

The Bit Error Rates (BERs) for the ten channels were determined through error counting, and are displayed in Fig. 4(a). By utilizing the MIMO equalizer, all the ten channels

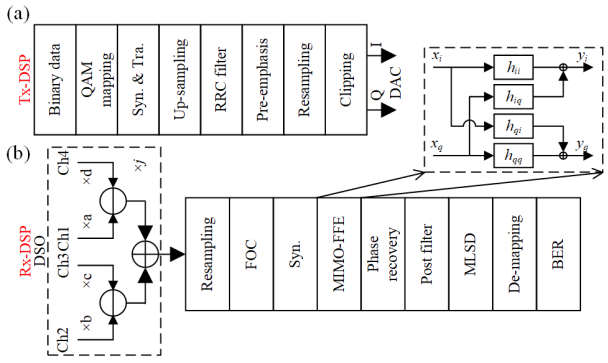

Fig. 3 DSP algorithms in the (a) transmitter, and (b) receiver, respectively.

maintained BERs below the 15% Soft-Decision Forward Error Correction (SD-FEC) threshold of 1.25×10^{-2}. This suggests that the MIMO equalizer presents superiority in compensating for the impairment caused by the IQ imbalance. Figs. 4(b~k) present ten constellation diagrams of the recovered DWDM-PDM 16-QAM signals. Overall, we achieved a nominal aggregate net data rate of 1.215Tb/s (calculated as 36 GBaud × 4 bit per symbol × 5 wavelengths × 2 polarizations × 0.971 (frame redundancy) / 1.07 (7% Forward Error Correction (FEC) overhead) = 1.215Tb/s).

V. Conclusion

We have proposed and demonstrated a 1.44-Tb/s silicon-integrated coherent receiver for DWDM and PDM transmission. As the light is mixed with the LO on the same wavelength, the signals of other wavelengths are shifted to high frequencies due to the beating effect and can be filtered out using an electrical low-pass filter. Moreover, the MIMO-FFE is employed to compensate IQ imbalance due to the non-uniform responsivities of GePDs. Compared to the traditional DWDM coherent receiver, AWG is not required, which saves a large footprint for the integrated coherent receiver. In the experiment, the 1.44-Tb/s 16-QAM 36-GBaud signals on five wavelengths and two polarizations are successfully recovered, with all BERs below the 15% SD-FEC threshold of 1.25×10^{-2}. However, this solution comes at the cost of a sacrificed SNR, requiring 6.9 dB more additional optical power to achieve the same SNR, and is more suitable for high-capacity short-range optical communication systems with high integration-level requirements. By adopting a more compact layout or reducing the sizes of the metal pads in the coherent receiver chip, we can further reduce the footprint of DWDM-PDM coherent receivers.

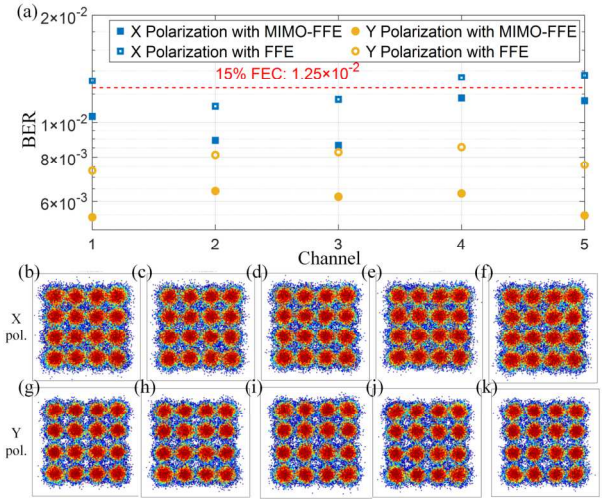

Fig. 4 (a) The calculated BERs of 36-GBaud 16-QAM signals for ten channels. (b~k) Recovered DWDM-PDM 16-QAM

References

[1] A. Chralyvy, "Plenary paper: The coming capacity crunch." 2009 35th European Conference on Optical Communication, pp. 1-1, 2009.

[2] R. W. Tkach, "Scaling Optical Communications for the Next Decade and Beyond," Bell Labs Technical Journal, vol. 14, no. 4, pp. 3-9, Win, 2010.

[3] A. D. Ellis, F. C. G. Gunning, B. Cuenot, T. C. Healy, E. Pincemin, and Ieee, "Towards 1TbE using Coherent WDM." OECC/ACOFT 2008-Joint Conference of the Opto-Electronics and Communications Conference and the Australian Conference on Optical Fibre Technology. IEEE, pp. 1-4, 2008.

[4] C. R. Doerr, L. L. Buhl, Y. Baeyens, R. Aroca, S. Chandrasekhar, X. Liu, L. Chen, and Y. K. Chen, "Packaged Monolithic Silicon 112-Gb/s Coherent Receiver," IEEE Photonics Technology Letters, vol. 23, no. 12, pp. 762-764, Jun, 2011.

[5] Y. J. Xia, L. Valenzuela, A. Maharry, S. Pinna, S. Dwivedi, T. Hirokawa, J. Buckwalter, C. Schow, and Ieee, "A Fully Integrated O-band Coherent Optical Receiver Operating up to 80 Gb/s," IEEE Photonics Conference, pp. 1-2, 2021.

[6] S. H. An, Q. M. Zhu, J. C. Li, Y. Y. Ling, and Y. K. Su, "112-Gb/s SSB 16-QAM signal transmission over 120-km SMF with direct detection using a MIMO-ANN nonlinear equalizer," Optics Express, vol. 27, no. 9, pp. 12794-12805, Apr, 2019.

[7] Y. Nasu, T. Mizuno, R. Kasahara, and T. Saida, "Temperature insensitive and ultra wideband silica-based dual polarization optical hybrid for coherent receiver with highly symmetrical interferometer design," Optics Express, vol. 19, no. 26, pp. 112-118, Dec, 2011.

[8] S. Tsukamoto, D. S. Ly-Gagnon, K. Katoh, and K. Kikuchi, "Coherent demodulation of 40-Gbit/s polarization-multiplexed QPSK signals with 16-GHz spacing after 200-km transmission," 2005 Optical Fiber Communications Conference Post deadline Papers, PDP29 , 2005.

[9] J. Verbist, J. Zhang, B. Moeneclaey, W. Soenen, J. Van Weerdenburg, R. Van Uden, C. Okonkwo, J. Bauwelinck, G. Roelkens, and X. Yin, "A 40-GBd QPSK/16-QAM Integrated Silicon Coherent Receiver," Ieee Photonics Technology Letters, vol. 28, no. 19, pp. 2070-2073, Oct, 2016.

[10] P. M. Seiler, K. Voigt, A. Peczek, G. Georgieva, S. Lischke, A. Malignaggi, and L. Zimmermann, "Multiband Silicon Photonic ePIC Coherent Receiver for 64 GBd QPSK," Journal of Lightwave Technology, vol. 40, no. 10, pp. 3331-3337, May, 2022.

[11] G. Soma, S. Ishimura, R. Tanomura, T. Fukui, M. Ito, Y. Nakano, and T. Tanemura, "Integrated dual-polarization coherent receiver without a polarization splitter-rotator," Optics Express, vol. 29, no. 2, pp. 1711-1721, Jan, 2021.

[12] S. Yamanaka, Y. Ikuma, T. Itoh, Y. Kawamura, K. Kikuchi, Y. Kurata, M. Jizodo, T. Jyo, S. Soma, M. Takahashi, K. Tsuzuki, M. Nagatani, Y. Nasu, A. Matsushita, T. Yamada, and Ieee, "Silicon Photonics Coherent Optical Subassembly with EO and OE Bandwidths of Over 50 GHz," 2020 Optical Fiber Communication Conference, pp. Th4A-4, 2020.

[13] Y. Kurata, Y. Nasu, M. Tamura, R. Kasahara, S. Aozasa, T. Mizuno, H. Yokoyama, S. Tsunashima, and Y. Muramoto, "Silica-based PLC with heterogeneously-integrated PDs for one-chip DP-QPSK receiver," Optics Express, vol. 20, no. 26, pp. B264-B269, Dec, 2012.

[14] P. J. Winzer, and R. J. Essiambre, "Advanced optical modulation formats," Proceedings of the Ieee, vol. 94, no. 5, pp. 952-985, May, 2006.

[15] K. Kikuchi, "Digital coherent optical communication systems: fundamentals and future prospects," Ieice Electronics Express, vol. 8, no. 20, pp. 1642-1662, Oct, 2011.

[16] J. Wang, M. Kroh, A. Theurer, C. Zawadzki, D. Schmidt, R. Ludwig, M. Lauermann, Z. Y. Zhang, A. Beling, A. Matiss, C. Schubert, A. Steffan, N. Keil, and N. Grote, "Dual-quadrature coherent receiver for 100G Ethernet applications based on polymer planar lightwave circuit," Optics Express, vol. 19, no. 26, pp. 166-172, Dec, 2011.

[17] S. Tsunashima, F. Nakajima, Y. Nasu, R. Kasahara, Y. Nakanishi, T. Saida, T. Yamada, K. Sano, T. Hashimoto, H. Fukuyama, H. Nosaka, and K. Murata, "Silica-based, compact and variable-optical-attenuator integrated coherent receiver with stable optoelectronic coupling system," Optics Express, vol. 20, no. 24, pp. 27174-27179, Nov, 2012.

[18] T. Ohyama, I. Ogawa, H. Tanobe, R. Kasahara, S. Tsunashima, T. Yoshimatsu, H. Fukuyama, T. Itoh, Y. Sakamaki, Y. Muramoto, H. Kawakami, M. Ishikawa, S. Mino, and K. Murata, "All-in-One 112-Gb/s DP-QPSK Optical Receiver Front-End Module Using Hybrid Integration of Silica-Based Planar Lightwave Circuit and Photodiode Arrays," Ieee Photonics Technology Letters, vol. 24, no. 8, pp. 646-648, Apr, 2012.

[19] D. Po, L. Xiang, S. Chandrasekhar, L. L. Buhl, R. Aroca, Y. Baeyens, and C. Young-Kai, "224-Gb/s PDM-16-QAM modulator and receiver based on silicon photonic integrated circuits," 2013 Optical Fiber Communication Conference and Exposition and the National Fiber Optic Engineers Conference (OFC/NFOEC), pp. 1-3, 2013.

[20] C. Doerr, L. Chen, D. Vermeulen, T. Nielsen, S. Azemati, S. Stulz, G. McBrien, X. M. Xu, B. Mikkelsen, M. Givehchi, C. Rasmussen, and S. Y. Park, "Single-chip silicon photonics 100-Gb/s coherent transceiver," 2014 Optical Fiber Communications Conference and Exhibition (OFC), pp. Th5C-1, 2014.

[21] L. Chen, C. Doerr, R. Aroca, S. Y. Park, J. C. Geyer, T. Nielsen, C. Rasmussen, and B. Mikkelsen, "Silicon photonics for 100G-and-beyond coherent transmissions," 2016 Optical Fiber Communications Conference and Exhibition (OFC), pp. Th1B-1, 2016.

[22] Y. X. Zhu, F. Zhang, F. Yang, L. Zhang, X. K. Ruan, Y. P. Li, and Z. Y. Chen, "Toward Single Lane 200G Optical Interconnects With Silicon Photonic Modulator," Journal of Lightwave Technology, vol. 38, no. 1, pp. 67-74, Jan, 2020.

[23] P. Dong, X. Liu, S. Chandrasekhar, L. L. Buhl, R. Aroca, and Y. K. Chen, "Monolithic Silicon Photonic Integrated Circuits for Compact 100(+)Gb/s Coherent Optical Receivers and Transmitters," Ieee Journal of Selected Topics in Quantum Electronics, vol. 20, no. 4, Jul-Aug, 2014.

[24] C. R. Doerr, L. Zhang, P. J. Winzer, and Ieee, "Monolithic InP Multi-Wavelength Coherent Receiver," 2010 Conference on Optical Fiber Communication (OFC/NFOEC), collocated National Fiber Optic Engineers Conference, pp. 1-3, 2010.

[25] R. Kaiser, B. G. Saavedra, G. Cincotti, M. Irion, P. Mitchell, N. Psaila, G. Vollrath, M. Schell, and Ieee, "Integrated All-Optical 8-Channel OFDM/Nyquist-WDM Transmitter and Receiver for Flexible Terabit Networks," International Conference on Transparent Optical Networks-ICTON, pp. 1-4, 2015.

[26] W. Wang, D. D. Zou, S. Y. Chen, Z. H. Li, and F. Li, "2x2 MIMO Equalizer Enabled Transmitter Side IQ Imbalance Compensation for Optical Single Sideband Direct Detection System," Journal of Lightwave Technology, vol. 40, no. 7, pp. 1914-1920, Apr, 2022.

[27] Z. Wang, X. Li, J. Li, J. Shen, Y. Zhang, and Y. Su, "Multi-carrier Tb/s Silicon Photonic Coherent Receiver," Science China Information Sciences, under review.

[28] P. Cheben, J. H. Schmid, A. Delage, A. Densmore, S. Janz, B. Lamontagne, J. Lapointe, E. Post, P. Waldron, and D. X. Xu, "A high-resolution silicon-on-insulator arrayed waveguide grating microspectrometer with submicrometer aperture waveguides," Optics Express, vol. 15, no. 5, pp. 2299-2306, Mar, 2007.

[29] Y. He, S. H. An, X. F. Li, Y. T. Huang, Y. Zhang, H. S. Chen, Y. K. Su, and Ieee, "Record high-order mode-division-multiplexed transmission on chip using gradient-duty-cycle subwavelength gratings," Optical Fiber Communication Conference, pp. F3A-2, 2021.

[30] S. T. Le, K. Schuh, R. Dischler, F. Buchali, L. Schmalen, and H. Buelow, "Beyond 400 Gb/s Direct Detection Over 80 km for Data Center Interconnect Applications," Journal of Lightwave Technology, vol. 38, no. 2, pp. 538-545, Jan, 2020.